

# A 0D thermochemical global model for the breakdown and the post discharge stages of a pulsed electrical discharge formed directly in water

B. Dufour<sup>1</sup>, C. Rond<sup>1</sup>, A. Vega<sup>1</sup> et X. Duten<sup>1</sup>

<sup>1</sup>LSPM – CNRS UPR3407, 99 avenue Jean-Baptiste Clément, Villetaneuse, France

**Abstract:** A 0D thermochemical global model of a pulsed electrical discharge formed directly in water has been developed. This work models the breakdown and the post breakdown stages but does not include the pre-breakdown stage. The chemical model of the gas phase includes 44 species involved in more than 500 reactions. The concentration is determined for each species, as well as the electron and gas temperatures. The detailed chemistry and the diffusion phenomena are also highlighted by the model.

**Keywords:** plasma-liquid, global model, non-equilibrium plasma

## 1. Introduction

In the past decades, plasmas in (and in contact) with liquids have been mainly studied for the breakdown of dielectric liquids within the framework of high-voltage switching [1]. More recently, it has been proposed to use these discharge types in water. This resurgence of interest is linked to emerging applications like nanomaterial synthesis, waste water treatment [2-3], plasma medicine [4], chemical synthesis [5-6], etc.

Pulsed direct liquid discharges are often generated by high voltage pulses since they need a fast breakdown process. Usually, such processes are achieved using high electric fields. Pulsed excitation is frequently obtained by discharging a capacitor with a very short rise-time switch leading to nanosecond or microsecond pulsed discharges [7].

This type of discharge leads to the establishment of filamentary luminous conductive gaseous channels, the so-called “streamers”. When these streamers span the inter-electrode gap, electrical breakdown in the liquid occurs which results in high electrical current, intense light emission and shock wave formation [7]. So one can split the full process in 3 time-based stages (illustrated in Fig.1): (i) the pre-breakdown which includes the initiation and the propagation of the streamers. (ii) Irrespective of the mechanisms involved during the initiation and the propagation phases, once the streamers have spanned the inter-electrode gap a highly ionized vapour channel is formed: the discharge filament. This stage is called the breakdown. This highly luminous plasma channel results from high energy electrons which involve strong dissociation and ionization processes. If one continues to inject energy, the discharge will be sustained. (iii) In the other case once the energy injection has stopped, as in pulsed regime, the discharge will extinguish because there won't be enough energy to maintain the ionization mechanisms inside the discharge filament previously created, it represents the post breakdown.

Despite the numerous experimental works performed in the frame of plasma-liquid interactions [8–12], the comprehension of the involved processes remains poor.

That's why there is a need for models in order to improve the understanding of the phenomenon involved in these types of discharges.

Some authors have developed physical models in order to simulate the discharge development and in particular streamer propagation. This approach has been made for uniform liquids [13], liquids with dissolved micro-bubbles [14], or even for discharges initiated inside existing bubbles immersed in liquids [15]. Other authors have developed chemical kinetics model data sets for gas phase plasmas for several types of mixtures. Among these, water vapour mixtures including humid air [16-17], He-H<sub>2</sub>O plasmas [18] but also Ar discharges containing humid air [19] can be mentioned.

This work will provide a comprehensive 0D thermochemical global model of the breakdown and post breakdown phases of an electrical discharge formed directly in water. The studied discharge has been also experimentally investigated within the laboratory [7], [20]. First, the experimental set-up is presented in section 2. Then, the approach and the hypothesis used in the model are detailed in section 3. It includes the characterization of the deposited power, the inclusion of the non-equilibrium and the description of the chemical model.

## 2. Experiment to model

The experiment to be modelled is presented in detail in [7] and [20]. The experimental set-up consists in a discharge cell containing de-ionized water at which we add sodium chloride in order to adjust the conductivity of the solution. Platinum electrodes (d=100µm) are in a pin-to-pin configuration, facing each other with an inter-electrode gap of 2 mm. The 30 kV pulsed power voltage source is composed of a 1 nF capacitor charged with a 30 W high-voltage source. Thanks to this configuration, we achieved pulses in the range of 6-14 kV amplitude and 100 µs to 1s duration. Pulses are positive with a fast rise time of about 30 ns followed by an exponential decay. Electrical measurements are registered through a 1 GHz bandwidth oscilloscope joined to a high voltage probe and

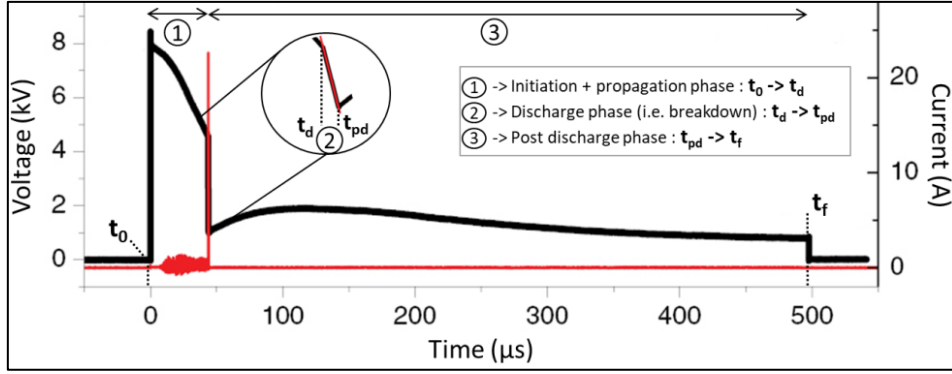


Fig. 1. Voltage and current signals monitored for an applied voltage of 9kV and a water conductivity of 100  $\mu\text{S}/\text{cm}$ .

a coaxial current shunt. Typical current and voltage waveform are shown in figure 1. Indeed, these electrical measurements provide some of the model's input data like the power deposited in the reactor.

### 3. Modelling approach

The model is consistent with those presented in [21] and [22] and is assumed to be quasi-homogeneous.

The discharge is divided into three distinct time-based stages. The first stage includes the initiation of the streamer and its propagation. It begins at  $t_0$ , the time at which the voltage pulse is applied, and ends at  $t_d$ , the time at which the breakdown occurs, that is to say when the streamers interconnect. This stage is not modelled in the present work. The second stage corresponds to the breakdown, also called discharge phase. Figure 2 shows a schematic diagram of the discharge phase as considered in the 0D model.

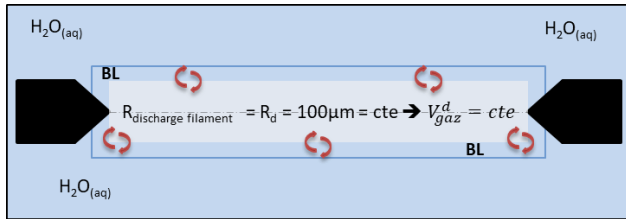


Fig. 2. Schematic of the discharge phase. “BL” means Boundary Layer and the red arrows represent the diffusion processes which take place between the discharge filament and the liquid BL.

It begins at  $t_d$  when the streamers span the inter electrode gap causing an intense light emission as observed in [7]. This light suggests that ionization and strong excitation mechanisms take place within the gaseous discharge filament. This stage lasts a few thousands of nanoseconds, allowing the assumption of a constant gas volume. This hypothesis is also strengthened by experimental observations [7]. This short duration corresponds to the duration of the voltage drop which ends at  $t_{pd}$ . Given the narrowness of the signal, the current peak (in red) appears as a Dirac in figure 1. The third and last stage refers to the post breakdown phase whose

schematic is shown in figure 3. It begins at  $t_{pd}$  when the energy deposited becomes negligible and ends at  $t_f$ , the end of the pulse. During this stage the gaseous post discharge volume is no more constant but it shows a bubble dynamic dependence: the gas volume expands and contracts just as cavitation bubbles [23].

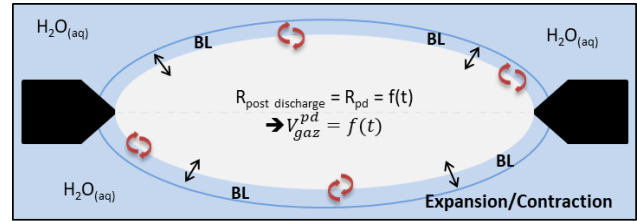


Fig. 3. Schematic of the post breakdown phase. “BL” means Boundary Layer and the red arrows represent the diffusion processes which take place between the post discharge volume and the liquid BL.

The present study is dedicated to the second and the third stage only. Given the schematics of the 2 stages studied (fig. 2 and fig. 3), each chemical species is characterized by the time evolution of its concentration in the gas phase,  $c_s$ , and in the liquid boundary layer surrounding it,  $c_s^{BL}$ . As reported hereafter the solved equations are the same for the breakdown and the post breakdown stages. The difference lays in the source terms, as the deposited energy, which are time-dependant.

This type of discharge is known to be in a strong thermal and chemical non-equilibrium. To represent the thermal non-equilibrium, the model includes two temperatures: electron kinetic translation temperature  $T_e$  and heavy species kinetic translation temperature  $T_g$ , also called gas temperature. Indeed, regarding the high pressure the number of collisions will be sufficient to consider that all vibrational levels are in equilibrium for each species of the model. Thus, we consider the vibrational temperature  $T_v$  to be equal to the gas temperature  $T_g$ . The rotational temperature of heavy species  $T_{rot}$  is also considered to be equal to the gas temperature as collisions between heavy species are very efficient for rotational transitions.

The energy deposited during one discharge is estimated using voltage and current measurements (shown in fig. 1) by integrating current-voltage product over the discharge duration, that is to say  $\int_{t_0}^{t_f} U(t) \times i(t) dt$ . For this calculation, we assume that the energy is uniformly deposited in the discharge filament volume  $V_{gas}^d$  only during the breakdown phase which allows us to calculate the power density simply dividing the absorbed power by the volume of the discharge filament which is assumed to be constant. As a first approximation, we will consider that the breakdown stage is the only period of time during which the power is deposited. This stage is distinguished from the post breakdown stage in which the power density is considered negligible. The electron energy distribution function (EEDF) is assumed to be Maxwellian in a first approximation because of the high prevailing pressure. Then, we can deduce the electron temperature  $T_e$

$$T_e = \frac{2 \langle E_e \rangle}{3 k_b} \quad (1)$$

where  $\langle E_e \rangle$  is the electron average energy and  $k_b$  the Boltzmann constant.

To calculate the electron average energy, an electron energy balance is used. This equation represents the difference between the total deposited energy and the portion of this energy consumed by collisional processes and is written:

$$\frac{dn_e \langle E_e \rangle}{dt} = P_{el} - \sum_{collisions} \alpha_c^e \nu_c E_c^{th} \quad (2)$$

where  $n_e$  is the electron density,  $P_{el}$  the space average of the time-dependant power density deposited in the discharge volume during one pulse,  $\alpha_c^e$  is the electron stoichiometric coefficient,  $\nu_c$  the reaction rate of the process "c" and  $E_c^{th}$  the threshold energy of the process "c". The second term in the right hand side of (2) represents the dissipation of the energy by electrons through collisional processes. As a matter of fact, the energy deposited will ionize the gas, heat the electrons and so consequently provoke electron-impact collisions. This leads to the primary discharge chemistry which produces the active species, species which will react again during the post breakdown phase.

Because of the strong heating of the electrons, the discharge will be in thermochemical disequilibrium. The chemical non-equilibrium is described using 44 species summarized in table 1.

Table 1. Species included in the global model

Species					
H	OH	H <sub>2</sub> O <sub>3</sub> <sup>+</sup>	O <sub>2</sub> <sup>+</sup>	H <sub>2</sub> O <sub>2</sub> <sup>-</sup>	O <sub>2</sub> (a) <sup>a</sup>
H <sub>2</sub>	H <sup>+</sup>	H <sub>5</sub> O <sub>2</sub> <sup>+</sup>	O <sub>4</sub> <sup>+</sup>	H <sub>3</sub> O <sub>2</sub> <sup>-</sup>	O <sub>2</sub> (b) <sup>a</sup>
H <sub>2</sub> O	H <sub>2</sub> <sup>+</sup>	H <sub>7</sub> O <sub>3</sub> <sup>+</sup>	OH <sup>+</sup>	H <sub>5</sub> O <sub>3</sub> <sup>-</sup>	OH(A)

HO <sub>2</sub>	H <sub>3</sub> <sup>+</sup>	H <sub>9</sub> O <sub>4</sub> <sup>+</sup>	H <sup>-</sup>	H(n=2)	e <sup>-</sup>
H <sub>2</sub> O <sub>2</sub>	HO <sub>2</sub> <sup>+</sup>	H <sub>11</sub> O <sub>5</sub> <sup>+</sup>	O <sup>-</sup>	H(n=3)	
O	H <sub>2</sub> O <sup>+</sup>	H <sub>13</sub> O <sub>6</sub> <sup>+</sup>	O <sub>2</sub> <sup>-</sup>	H(n=4)	
O <sub>2</sub>	H <sub>3</sub> O <sup>+</sup>	H <sub>15</sub> O <sub>7</sub> <sup>+</sup>	O <sub>3</sub> <sup>-</sup>	O( <sup>1</sup> D)	
O <sub>3</sub>	H <sub>4</sub> O <sub>2</sub> <sup>+</sup>	O <sup>+</sup>	OH <sup>-</sup>	O( <sup>1</sup> S)	

<sup>a</sup> O<sub>2</sub>(a) accounts for O<sub>2</sub>(a<sup>1</sup>Δ<sub>g</sub>) and O<sub>2</sub>(b) accounts for O<sub>2</sub>(b<sup>1</sup>Σ<sub>g</sub><sup>+</sup>)

These species are involved in more than 500 reactions whose types of processes are listed in table 2.

Table 2. Types of reactions included in the model

Excitation	De-excitation
Ionization	Attachment
Dissociation	Recombination
Association	Neutralization
Elastic scattering	Momentum transfer
Electron impact electronic excitation	Radiation

In the present model we assume to have purely diffusive transport phenomena because of the absence of mechanical stirring (gas flow, stirrer ...), and so of forced convection, in our reactor. However, the Peclet number being quite high in liquids, the fully diffusive transport approximation is only valid for a small inter-electrode gap where we can neglect the advective motion of the liquid. Moreover, even if the total density and gas temperature gradients become high enough to generate strong free convection phenomenon, characteristic times involved are too short to establish free convection. One can estimate the molar flux from the difference of concentration between the gas volume  $V_{gas}$  and the associated liquid boundary layer (cf. fig. 2 and fig. 3). Then, one can deduce the diffusion fluxes.

$$J_s = -D_s \times \frac{c_s^{BL} - c_s}{L_c^{dif}} \quad (3)$$

where  $D_s$  is the diffusion coefficient for the species "s" and  $L_c^{dif}$  is the characteristic length of diffusion. Concerning the charged species, we use the ambipolar diffusion coefficient  $D_a = D_s(1 + T_e/T_g)$ . The diffusion process will be different during the breakdown and the post breakdown. Consequently, the diffusion coefficient  $D_s$  will also be different between these 2 stages.

Considering all the assumptions of the model, one can deduce the species continuity equations solved for each heavy species "s" including electrons in order to get the species concentrations during the two stages of the discharge.

$$\frac{dc_s}{dt} = W_s + R_s \quad (4)$$

where  $W_s$  denotes the production rate for species “s” in the gas phase,  $R_s$  denotes the rate of concentration change due to diffusion processes for species “s” which is given by

$$R_s = -J_s \frac{S_l}{V_{gas}} \quad (5)$$

where  $V_{gas}$  represents the gas volume and  $S_l$  the lateral surface of the gas volume.

Regarding the production rates, we have:

$$W_s = M_s \times \sum_{j=1}^{N_r} [k_j (v_{sj}^{(2)} - v_{sj}^{(1)}) (\prod_{k=1}^{N_s} (c_k)^{v_{kj}})] \quad (6)$$

where  $M_s$ ,  $N_r$ ,  $N_s$ ,  $k_j$ ,  $v_{sj}$ ,  $v_{kj}$ ,  $c_k$  are respectively the molecular weight of species “s”, the number of reactions included in the model, the number of species included in the model, the rate of chemical reaction “j”, the stoichiometric ratios of the product, the stoichiometric ratio of the reactants, the concentration of the species “k” in the gas volume  $V_{gas}$ . Both of these source terms will be different depending on the stage and will be formulated accordingly.

The kinetic model is numerically integrated with the Livermore solver for ordinary differential equations, LSODE [24]. This choice is due to the stiffness of our problem and in particular the high non-linearity of the differential equation set. Indeed, LSODE solver uses the backward differentiation formula (BDF) method, also called the Gear method, which has the property of stiff stability. This stiffness comes from the concentrations of the rapid chemical components in the plasma which quickly decay to very small values.

#### 4. Conclusion

The kinetics of a H<sub>2</sub>O discharge has been investigated. Species concentration, electron and gas temperatures are under investigation in order to detail the thermo-chemical behaviour of a pin-to-pin electrical discharge in water. The diffusion fluxes between the gas volume and the liquid boundary layer are calculated during the breakdown and the post breakdown stages. Regarding the size of the kinetic scheme, further work has still to be done in order to reduce it. We would like to identify the most significant pathways for the production and the destruction of species of interest in order to improve our experimental process. This work is currently under development using the PumpKin software [25]

#### 5. References

- [1] E. Kuffel, W. S. Zaengl, et J. Kuffel, 2. ed., reprint. Amsterdam: Newnes, Elsevier, 2008.
- [2] V. M. Bystritskii, T. K. Wood, Y. Yankelevich, S. Chauhan, D. Yee, et F. Wessel, in *Digest of Technical Papers. 11th IEEE International Pulsed Power Conference (Cat. No.97CH36127)*, Baltimore, MA, USA, 1997, vol. 1, p. 79-84.
- [3] J. Foster, B. S. Sommers, S. N. Gucker, I. M. Blankson, et G. Adamovsky, *IEEE Trans. Plasma Sci.*, vol. 40, n° 5, p. 1311-1323, mai 2012.
- [4] A. M. Lietz et M. J. Kushner, *J. Phys. Appl. Phys.*, vol. 49, n° 42, p. 425204, oct. 2016.
- [5] P. Sunka et al., *Plasma Sources Sci. Technol.*, vol. 8, n° 2, p. 258-265, mai 1999.
- [6] S. Hamaguchi, K. Ikuse, et T. Kanazawa, in *Proceedings of the 12th Asia Pacific Physics Conference (APPC12)*, Makuhari, Japan, 2014.
- [7] C. Rond et al., *J. Phys. Appl. Phys.*, vol. 51, n° 33, p. 335201, août 2018.
- [8] A. Starikovskiy, Y. Yang, Y. I. Cho, et A. Fridman, *Plasma Sources Sci. Technol.*, vol. 20, n° 2, p. 024003, avr. 2011.
- [9] A. Yamatake, D. M. Angeloni, S. E. Dickson, M. B. Emelko, K. Yasuoka, et J.-S. Chang, *Jpn. J. Appl. Phys.*, vol. 45, n° 10B, p. 8298-8301, oct. 2006.
- [10] M. Pekker et M. N. Shneider, *J. Phys. Appl. Phys.*, vol. 48, n° 42, p. 424009, oct. 2015.
- [11] J. Qian et al., *J. Appl. Phys.*, vol. 97, n° 11, p. 113304, juin 2005.
- [12] O. Lesaint, *J. Phys. Appl. Phys.*, vol. 49, n° 14, p. 144001, avr. 2016.
- [13] N. Y. Babaeva et G. V. Naidis, *Tech. Phys. Lett.*, vol. 25, n° 2, p. 91-94, févr. 1999.
- [14] J. Qian, R. P. Joshi, E. Schamiloglu, J. Gaudet, J. R. Woodworth, et J. Lehr, *J. Phys. Appl. Phys.*, vol. 39, n° 2, p. 359-369, janv. 2006.
- [15] N. Y. Babaeva et M. J. Kushner, *J. Phys. Appl. Phys.*, vol. 42, n° 13, p. 132003, juill. 2009.
- [16] H. Milloy, I. Reid, et R. Crompton, *Aust. J. Phys.*, vol. 28, n° 2, p. 231, 1975.
- [17] H. Hingana, .
- [18] D. X. Liu, P. Bruggeman, F. Iza, M. Z. Rong, et M. G. Kong, *Plasma Sources Sci. Technol.*, vol. 19, n° 2, p. 025018, avr. 2010.
- [19] W. V. Gaens et A. Bogaerts, *J. Phys. Appl. Phys.*, vol. 46, n° 27, p. 275201, juill. 2013.
- [20] C. Rond, J. M. Dese, N. Fagnon, X. Aubert, A. Vega, et X. Duten, *J. Phys. Appl. Phys.*, vol. 52, n° 2, p. 025202, janv. 2019.
- [21] S. Medodovic et B. R. Locke, *J. Phys. Appl. Phys.*, vol. 42, n° 4, p. 049801-049801, févr. 2009.
- [22] M. Redolfi, N. Aggadi, X. Duten, S. Touchard, S. Pasquiers, et K. Hassouni, *Plasma Chem. Plasma Process.*, vol. 29, n° 3, p. 173-195, juin 2009.
- [23] A. Hamdan, C. Noel, F. Kosior, G. Henrion, et T. Belmonte, *J. Acoust. Soc. Am.*, vol. 134, n° 2, p. 991-1000, août 2013.
- [24] K. Radhakrishnan et A. C. Hindmarsh, NASA, Office of Management, Scientific and Technical Information Program, 1993.
- [25] A. H. Markosyan, A. Luque, F. J. Gordillo-Vázquez, et U. Ebert, *Comput. Phys. Commun.*, vol. 185, n° 10, p. 2697-2702, oct. 2014.